HHS Public Access

Author manuscript

Dermatol Clin. Author manuscript; available in PMC 2017 August 24.

Published in final edited form as:

Dermatol Clin. 2016 October ; 34(4): 497–504. doi:10.1016/j.det.2016.05.012.

In Vivo and Ex Vivo Confocal Microscopy for Dermatologic and Mohs Surgeons

Caterina Longo, MD, PhD[a,*], **Moira Ragazzi, MD**[b], **Milind Rajadhyaksha, PhD**[c], **Kishwer Nehal, MD**[c], **Antoni Bennassar, MD**[d], **Giovanni Pellacani, MD**[e], and **Josep Malvehy Guilera, MD, PhD**[d]

[a]Skin Cancer Unit, Arcispedale Santa Maria Nuova-IRCCS, viale Risorgimento 80, Reggio Emilia 42100, Italy

[b]Pathology Unit, Arcispedale Santa Maria Nuova-IRCCS, viale Risorgimento 80, Reggio Emilia 42100, Italy

[c]Dermatology Service, Memorial Sloan Kettering Cancer Center, 160 East 53rd Street, New York, NY 10022, USA

[d]Melanoma Unit, Dermatology Department, Hospital Clinic and Institut d'Investigacions Biomediques August Pi I Sunyer, Barcelona, Spain

[e]Dermatology Unit, UniMore, Modena, Italy

Keywords

Confocal microscopy; In vivo; Ex vivo; Mohs surgery

INTRODUCTION

Micrographic Mohs surgery is a precise and complete excision of a skin cancer guided by the examination of margins with frozen histopathology during surgery. It was developed several years ago and is still applied in clinical dermatologic settings especially for some cancers, such as basal cell carcinoma (BCC) and squamous cell carcinoma (SCC). However, this technique has some drawbacks: the preparation of histopathology is labor intensive and time consuming, and multiple serial excisions are often necessary to achieve cancerfree margins, with frozen tissue preparation requiring 20 to 45 minutes for each stage. Furthermore, there are cost-related issues.

Confocal microscopy has been introduced in clinical settings in the last decades as a revolutionary tool capable of offering a quasi-histologic view of a given skin tumor in a few minutes.[1–4] Confocal microscopes works with two different modalities: in reflectance mode and in fluorescence mode. In reflectance confocal microscopy (RCM) contrast is achieved because of different refractive indices of cell structures and organelles, such as keratin and melanin; these serve as "endogenous chromophores" in the reflection-mode because of a

*Corresponding author. longo.caterina@gmail.com.

The authors have no conflicts of interest to disclose.

higher refractive indices compared with water. This device is used in vivo at the patient's bedside.

Fluorescence confocal microscopy (FCM) uses as fluorescent agents several fluorophores among which acridine orange is one of the most commonly used in the clinical setting. This tool works in the ex vivo setting on freshly excised specimens.[1–3]

Both modalities have been applied for Mohs surgery in skin cancer diagnosis and margin assessment. This article reviews the application of in vivo and ex vivo confocal microscopy in the Mohs surgery setting.

IN VIVO APPLICATIONS OF REFLECTANCE CONFOCAL MICROSCOPY

In vivo RCM has been applied at the patient's bedside for lateral margin detection in BCC and lentigo maligna (LM), because of its capability of exploring the skin at the cellular level, enabling the identification of tumor characteristics.

Basal Cell Carcinoma

Regarding BCC margin assessment, Venturini and colleagues[5,6] proposed a new feasible procedure for presurgical evaluation. Briefly, after the application of topical anesthesia, the lesion is analyzed by dermoscopy. Next, clear borders, approximately 2 mm from identifiable structures, are drawn with a dermographic pen, according to dermoscopic evaluation of the lesion. In the case of ill-defined tumor margins, a superficial cut with a lancet is made in correspondence with the presumed clear margin based on dermoscopy. Then, RCM is carried out by means of Vivascope 1500 (Mavig, Munchen, Germany), placing the cut at the center of the imaged area. A series of mosaics up to 4 × 4 mm in size at different depths are acquired to explore the area inside and outside the superficial cut and to determine if the margin is tumor-free (RCM-negative border corresponding to no BCC tumor features outside the cut or within 2 mm of the cut) or involved (RCM-positive border corresponding to BCC tumor features outside the cut or within 2 mm of the cut). In the case of an RCM-positive border, to perform radical excision, a clear border is redefined on RCM images and transposed onto the skin according to its direction and distance from the superficial cut.

In this study, RCM evaluation showed BCC foci beyond the presurgical mark in 3 of 10 (30%) lesions, demonstrated by polarization of elongated nuclei along the same axis of orientation, dark silhouettes, and increased dermal vasculature with tortuous and ectatic blood vessels. Thus, this method could represent a valid and relatively fast approach for lateral margin detection in BCC. However, because of the limited depth laser penetration, deep tumor margin cannot be assessed and this is crucial for sclerosing BCC or deeply infiltrating tumors.

Another and different application of in vivo RCM involves the use of video mosaicking for rapid detection of residual tumor directly in the surgical wounds on patients.[7] A recent study used this approach on 25 patients, using aluminum chloride for nuclear contrast. Basically, imaging is performed in quadrants in the wound to simulate the Mohs surgeon's

examination of pathology. Images and videos of the epidermal and dermal margins are acquired and bright nuclear morphology can be identified at the epidermal margin and detectable in residual nonmelanoma skin cancer tumors. Although this was a pilot feasibility study, intraoperative RCM imaging was found to be useful for the detection of residual tumor directly on patients during Mohs surgery. However, for routine clinical utility, a stronger tumor-to-dermis contrast may be necessary, and a smaller microscope head with an automated approach for imaging the entire wound in a rapid and controlled manner.

Lentigo Maligna

Delineating margins of LM preoperatively is often extremely challenging because of the pigmentation of the sun-damaged background and the intrinsic early changes of the tumor that is composed of single atypical melanocytic proliferation. Guitera and colleagues[8] in a subset of 29 patients have explored the use of in vivo RCM for LM mapping. A detailed procedure has been developed to ensure a presurgical definition of clear margins. When the lesion was visible clinically or on dermoscopy, the RCM field of view is centered in the middle of the lesion. Confocal images are obtained in four radial directions for margin determination until no evidence of LM is seen. The margins are explored in only four directions because of the time necessary to capture each mosaic. The histopathologic findings and diagnosis correlated with the RCM features in nearly all cases. In this study, there were four false-positive sites (diagnosed as an LM area by the LM score on RCM and not confirmed by pathologic findings) and five false-negative sites (diagnosed as LM by histopathologic study but not by the RCM assessment). Thus, this method is a reliable and easy method for presurgical margin assessment of LM.

Another interesting way to outline LM margin is the so-called “spaghetti” technique.[9] Marking is done at the visual limits of the LM, based on clinical and dermoscopy examination. The following evaluations are performed circumferentially, moving closer by 5 mm to the visual limits if the analysis is negative and moving away by 5 mm if malignant cells are identified. This spacing of 5 mm corresponds to the size of the tip of the Vivascope 3000 camera (Mavig). When applied to the skin, this tip creates a temporary footprint that serves as a transitional benchmark for the next exploration, with the tip applied adjacent to the mark left by the previous exploration. Then, a mark is made on the analyzed area using a dermographic pen as a dot in the center of the skin foot-print of the camera after quickly mopping up the interface oil used for the RCM examination. These dots are interconnected by a line, drawn using a dermographic pen and then stained with a solution of fuchsin ink to avoid any possible deletion during preoperative disinfection of the skin. The outline of the lesion is marked. This method has been used only on 33 cases and thus limited conclusions can be drawn; however, the “spaghetti” technique allows accurate definition of the surgical margins of LM, with a low rate of multiple excisions.

Besides LM mapping, RCM has been successfully applied to accurately monitor the response of LM to nonsurgical treatment with topical imiquimod.[10] RCM identified 70% of all responders with no false-negative results, and when compared with histopathology, there was no significant difference in evaluating the response to imiquimod.

EX VIVO APPLICATIONS OF FLUORESCENCE CONFOCAL MICROSCOPY

Ex vivo FCM is used on freshly excised tumors in the operating room. Different fluorophores, such as fluorescein, Nile blue, patent blue, methylene blue, and acridine orange, can be used at different wavelengths. However, acridine orange is one of the most commonly used because of its capability to provide an excellent contrast. Confocal mosaics are acquired using an ex vivo fluorescence confocal microscope (Vivascope 2500, Mavig). The laser illumination wavelength is 488 nm. The depth is manually adjusted to image the surface. Imaging is with a 30 × 0.9 numerical aperture water immersion lens, which provides optical sectioning of approximately 1.5 μm and resolution of approximately 0.4 μm at the 488-nm wavelength. Acridine orange (0.6 mM, 10–20 seconds) is used as the contrast agent.

Basal Cell Carcinoma

FCM images provides an excellent correlation with conventional frozen sections while adding more information regarding fat tissue and other structures that can be altered by tissue processing in classic Mohs surgery.

A set of traditional histologic classic and new criteria has been developed to guide the reading and interpretation of the gray scale mosaics.[11–28] FCM criteria include the presence of the following:

1. *Fluorescence.* Presence of fluorescence was determined when bright images were seen on the screen. Fluorescence corresponds to nucleated cells stained with acridine orange. Areas of higher fluorescence consistently showed nuclear morphology compared with a darker appearing background of dermis (Fig. 1); fluorescence is typically seen as forming structures/aggregates.
2. *Tumor demarcation* (Fig. 2). Tumor shape corresponds to distinct histopathology subtypes.
3. *Nuclear crowding.* Nuclear crowding was determined when the nuclear density was higher than that of the surrounding epidermis and adnexal structures.
4. *Peripheral palisading.* Palisading is described, similar to that seen in frozen histology, by the prominent tendency of the outermost layer of basal cells to be arranged in a parallel-polarized way along the periphery of the BCC tumor. This is seen mainly in nodular subtypes of BCCs (Fig. 3).
5. *Clefting.* Hypofluorescent dark-appearing space surrounding basaloid islands partially outlines the islands in micronodular and infiltrative subtypes of BCCs; it is more evident in superficial and nodular tumors.
6. *Nuclear pleomorphism.* Nuclear pleomorphism is a deviation from the normal round or oval shapes of nuclei present in normal keratinocytes.
7. *Increased nucleus/cytoplasm ratio.* BCC nests are seen as crowded masses of elongated heterogeneous nuclei with poor or absent cytoplasm.

8. *Stroma.* Tumoral stroma is the modified dermis surrounding the BCC nests. When viewed in FCM mosaics, the stroma is seen as more densely nucleated dermis, as fluorescent dots and filaments within a dark-appearing background.

Furthermore, distinct BCC subtypes reveal specific morphologic aspects. Superficial BCCs show a proliferation of atypical basaloid cells that form an axis parallel to the epidermal surface, are extensions from the dermal-epidermal junction, and demonstrate slitlike retraction of the palisaded basal cells from the subjacent stroma (cleft-like spaces). Nodular BCCs reveal small to large nodules with peripheral palisading and clefting, whereas the micronodular subtype shows monotonous small round and well-defined islands with roughly the same shape and contour. Infiltrative BCCs are the most challenging tumor because they appear as columns and cords of basaloid cells one to two cells thick with sharp angulation, enmeshed in a densely collagenized stroma; palisading and clefting are not always present.

Several studies have been conducted to assess the value of FCM for BCC margin assessment (Table 1). A study conducted by Bennassar and colleagues[28] on 80 BCCs using these FCM criteria demonstrated an overall sensitivity and specificity of detecting residual BCC of 88% and 99%, respectively. Moreover, the new technique reduced by almost two-thirds the time invested when compared with the conventional processing of frozen sections.[29] Several pitfalls may occur when evaluating FCM mosaics.[30] In particular, tiny and angulated cords and strands of fluorescent cells that are typically found in infiltrative BCCs can be more difficult to recognize. Furthermore, it is difficult to distinguish the infiltrative cords from the surrounding stroma, although the latter showed no tendency to cluster. Another possible pitfall is caused by the presence of several sebaceous glands that may be confused with BCC islands. However, the former showed no palisading, less fluorescence, and the presence of a centrally located nucleus compared with the tumors.

Squamous Cell Carcinoma

Few preliminary reports describe the feasibility of FCM for SCC diagnosis and margin assessment. Longo and colleagues[31] defined the FCM criteria to grade SCC tumors. This pilot study demonstrated that the presence of a well-defined tumor silhouette, numerous keratin pearls, keratin formation, and scarce nuclear pleomorphism on FCM images were correlated with the diagnosis of well-differentiated SCC (Fig. 4). Conversely, an ill-defined tumor silhouette, paucity or absence of keratin pearls, and marked nuclear pleomorphism was observed in poorly differentiated tumors. SCCs that were moderately differentiated revealed an intermediate pattern of growth with presence of keratin formation.

OTHER TUMORS

FCM has been used to assess the margins during micrographic mohs surgery (MMS) of eccrine syringomatous carcinoma.[32] On FCM the tumor appears highly fluorescent. Epidermis is spared of any neoplastic proliferation, whereas neoplastic cords of monomorphous fluorescent cells can be seen in the dermis. Those structures are similar to eccrine gland tubular structure.

SUMMARY

The need of defining skin cancer margins for a more accurate surgical excision has fueled the exploration of confocal microscopy in this special setting. In vivo and ex vivo confocal microscopy has been used with the great advantage of saving time and providing good diagnostic accuracy. For both techniques intense and dedicated training is required to learn how to use the device and even more relevant, how to interpret the images. For the near future we envision the routine application of confocal microscopy in the Mohs surgery setting.

Acknowledgments

Funding: Dr C. Longo and Prof G. Pellacani were partially funded by Research Project NET-2011-02347213, Italian Ministry of Health.

References

1. Rajadhyaksha M, Menaker G, Flotte T, et al. Confocal examination of nonmelanoma cancers in thick skin excisions to potentially guide Mohs micrographic surgery without frozen histopathology. J Invest Dermatol. 2001; 117:1137–43. [PubMed: 11710924]
2. Chung VQ, Dwyer PJ, Nehal KS, et al. Use of ex vivo confocal scanning laser microscopy during Mohs surgery for nonmelanoma skin cancers. Dermatol Surg. 2004; 30:1470–8. [PubMed: 15606734]
3. Patel YG, Nehal KS, Aranda I, et al. Confocal reflectance mosaicing of basal cell carcinomas in Mohs surgical skin excisions. J Biomed Opt. 2007; 12(3):034027. [PubMed: 17614735]
4. Longo C, Zalaudek I, Argenziano G, et al. New directions in dermatopathology: in vivo confocal microscopy in clinical practice. Dermatol Clin. 2012; 30(4):799–814. [PubMed: 23021059]
5. Venturini M, Gualdi G, Zanca A, et al. A new approach for presurgical margin assessment by reflectance confocal microscopy of basal cell carcinoma. Br J Dermatol. 2016; 174(2):380–5. [PubMed: 26498991]
6. Gualdi G, Venturini M, Zanca A, et al. Pre-surgical basal cell carcinoma margin definition: the SMART approach. J Eur Acad Dermatol Venereol. 2016; 30(3):474–6. [PubMed: 25413728]
7. Flores ES, Cordova M, Kose K, et al. Intraoperative imaging during Mohs surgery with reflectance confocal microscopy: initial clinical experience. J Biomed Opt. 2015; 20(6):61103. [PubMed: 25706821]
8. Guitera P, Moloney FJ, Menzies SW, et al. Improving management and patient care in lentigo maligna by mapping with in vivo confocal microscopy. JAMA Dermatol. 2013; 149(6):692–8. [PubMed: 23553208]
9. Champin J, Perrot JL, Cinotti E, et al. In vivo reflectance confocal microscopy to optimize the spaghetti technique for defining surgical margins of lentigo maligna. Dermatol Surg. 2014; 40(3): 247–56. [PubMed: 24447286]
10. Alarcon I, Carrera C, Alos L, et al. In vivo reflectance confocal microscopy to monitor the response of lentigo maligna to imiquimod. J Am Acad Dermatol. 2014; 71(1):49–55. [PubMed: 24725478]
11. Gareau DS, Patel YG, Li Y, et al. Confocal mosaicing microscopy in skin excisions: a demonstration of rapid surgical pathology. J Microsc. 2009; 233(1):149–59. [PubMed: 19196421]
12. SchUle D, Breuninger H, Schippert W, et al. Confocal laser scanning microscopy in micrographic surgery (three-dimensional histology) of basal cell carcinomas. Br J Dermatol. 2009; 161(3):698–700. [PubMed: 19575731]
13. Ziefle S, SchUle D, Breuninger H, et al. Confocal laser scanning microscopy vs 3-dimensional histologic imaging in basal cell carcinoma. Arch Dermatol. 2010; 146(8):843–7. [PubMed: 20713814]

14. Kaeb S, Landthaler M, Hohenleutner U. Confocal laser scanning microscopy-evaluation of native tissue sections in micrographic surgery. Lasers Med Sci. 2009; 24(5):819–23. [PubMed: 19277819]
15. Yaroslavsky AN, Barbosa J, Neel V, et al. Combining multispectral polarized light imaging and confocal microscopy for localization of nonmelanoma skin cancer. J Biomed Opt. 2005; 10(1): 14011. [PubMed: 15847592]
16. Al-Arashi MY, Salomatina E, Yaroslavsky AN. Multimodal confocal microscopy for diagnosing nonmelanoma skin cancers. Lasers Surg Med. 2007; 39(9):696–705. [PubMed: 17960751]
17. Gareau DS, Li Y, Huang B, et al. Confocal mosaicing microscopy in Mohs skin excisions: feasibility of rapid surgical pathology. J Biomed Opt. 2008; 13(5):054001. [PubMed: 19021381]
18. Gareau DS, Karen JK, Dusza SW, et al. Sensitivity and specificity for detecting basal cell carcinomas in Mohs excisions with confocal fluorescence mosaicing microscopy. J Biomed Opt. 2009; 14(3):034012. [PubMed: 19566305]
19. Karen JK, Gareau DS, Dusza SW, et al. Detection of basal cell carcinomas in Mohs excisions with fluorescence confocal mosaicing microscopy. Br J Dermatol. 2009; 160(6):1242–50. [PubMed: 19416248]
20. Bennassar A, Vilalta A, Carrera C, et al. Rapid diagnosis of two facial papules using ex vivo fluorescence confocal microscopy: toward a rapid bedside pathology. Dermatol Surg. 2012; 38(9): 1548–51. [PubMed: 22823541]
21. Abeytunge S, Li Y, Larson B, et al. Rapid confocal imaging of large areas of excised tissue with strip mosaicing. J Biomed Opt. 2011; 16(5):050504. [PubMed: 21639560]
22. Abeytunge S, Li Y, Larson B, et al. Confocal microscopy with strip mosaicing for rapid imaging over large areas of excised tissue. J Biomed Opt. 2013; 18(6):61227. [PubMed: 23389736]
23. Larson B, Abeytunge S, Seltzer E, et al. Detection of skin cancer margins in Mohs excisions with high-speed strip mosaicing confocal microscopy: a feasibility study. Br J Dermatol. 2013; 169:922–6. [PubMed: 23701464]
24. Gareau DS. Feasibility of digitally stained multimodal confocal mosaics to simulate histopathology. J Biomed Opt. 2009; 14(3):034050. [PubMed: 19566342]
25. Gareau DS, Jeon HS, Nehal KS, et al. Rapid screening of cancer margins in tissue with multimodal microscopy. J Surg Res. 2012; 178:533–8. [PubMed: 22721570]
26. Gareau D, Bar A, Snaveley N, et al. Tri-modal confocal mosaics detect residual invasive squamous cell carcinoma in Mohs surgical excisions. J Biomed Opt. 2012; 17(6):066018. [PubMed: 22734774]
27. Longo C, Ragazzi M, Castagnetti F, et al. Inserting ex vivo fluorescence confocal microscopy perioperatively in Mohs micrographic surgery expedites bedside assessment of excision margins in recurrent basal cell carcinoma. Dermatology. 2013; 227(1):89–92. [PubMed: 24008980]
28. Bennassar A, Carrera C, Puig S, et al. Fast evaluation of 69 basal cell carcinomas with ex vivo fluorescence confocal microscopy: criteria description, histopathological correlation, and interobserver agreement. JAMA Dermatol. 2013; 149(7):839–47. [PubMed: 23636776]
29. Bennassar A, Vilata A, Puig S, et al. Ex vivo fluorescence confocal microscopy for fast evaluation of tumour margins during Mohs surgery. Br J Dermatol. 2014; 170(2):360–5. [PubMed: 24117457]
30. Longo C, Rajadhyaksha M, Ragazzi M, et al. Evaluating ex vivo fluorescence confocal microscopy images of basal cell carcinomas in Mohs excised tissue. Br J Dermatol. 2014; 171(3):561–70. [PubMed: 24749970]
31. Longo C, Ragazzi M, Gardini S, et al. Ex vivo fluorescence confocal microscopy in conjunction with Mohs micrographic surgery for cutaneous squamous cell carcinoma. J Am Acad Dermatol. 2015; 73(2):321–2. [PubMed: 26183978]
32. Longo C, Ragazzi M, Gardini S, et al. Ex vivo fluorescence confocal microscopy of eccrine syringomatous carcinoma: a report of 2 cases. JAMA Dermatol. 2015; 151(9):1034–6. [PubMed: 26017696]

KEY POINTS

- Confocal microscopy is an optimal device that offers a nearly histologic view of skin tissue.
- In vivo confocal microscopy helps to outline lateral basal cell carcinoma margins with accuracy, although it has been tested on a limited set of patients.
- Ex vivo confocal microscopy is a valid alternative to conventional frozen section pathology for BCC margin assessment.

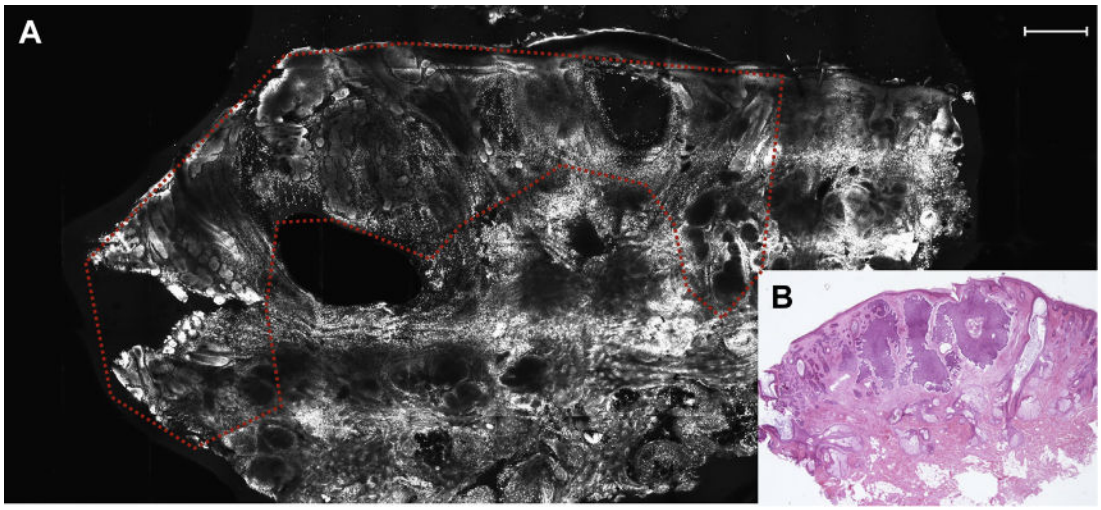

Fig. 1.

(*A*) Tumor silhouette of BCC was highlighted by higher fluorescence signal (*dashed line;* scale bar, 750 μm). (*B*) Nodular BCC on frozen section revealing an excellent correlation with FCM image in A (hematoxylin-eosin, original magnification 2×).

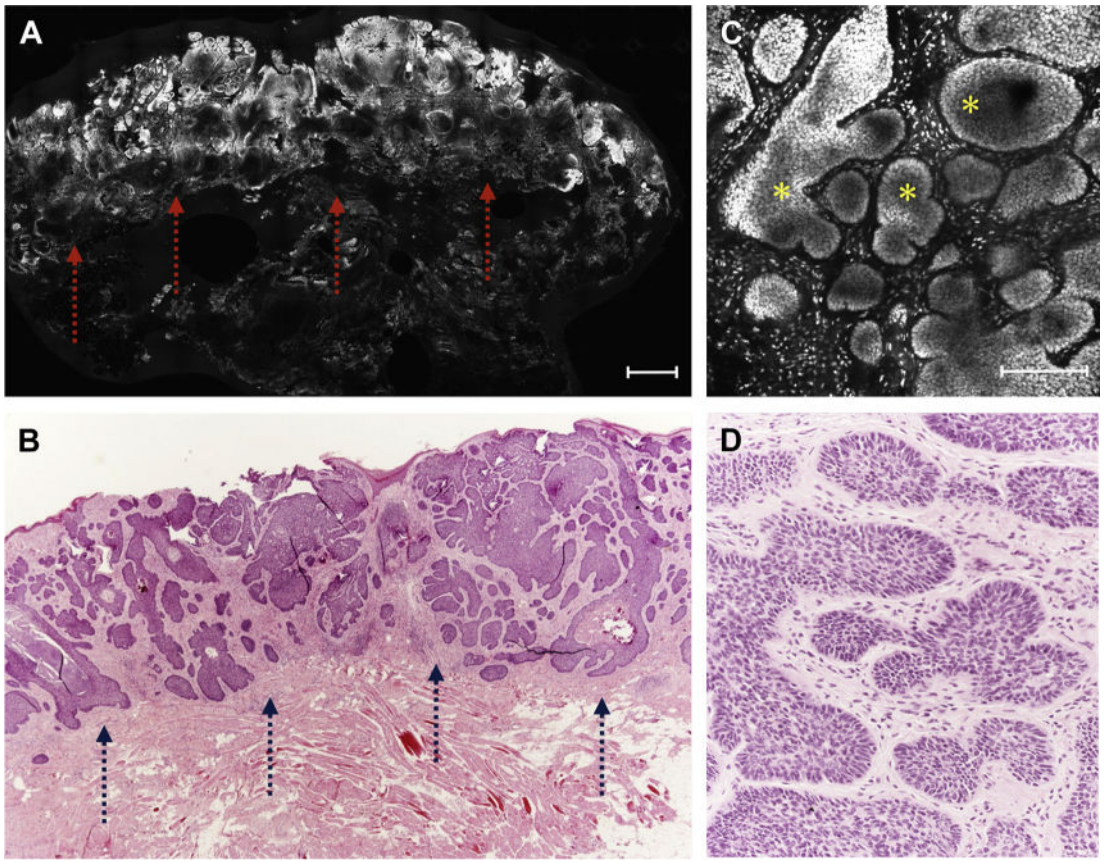

Fig. 2.

(*A*) Low-resolution FCM image showing a BCC tumoral proliferation (*arrows*; scale bar, 750 μm). (*B*) Stained section depicted an excellent correlation with FCM image (*arrows*) in *A* (hematoxylin-eosin, original magnification 2×). (*C*) High-resolution FCM image showed the presence of basaloid islands (*asterisks*) with peripheral palisading and clefting that corresponded to the ones seen on histology (*D*) (hematoxylin-eosin, original magnification 10×).

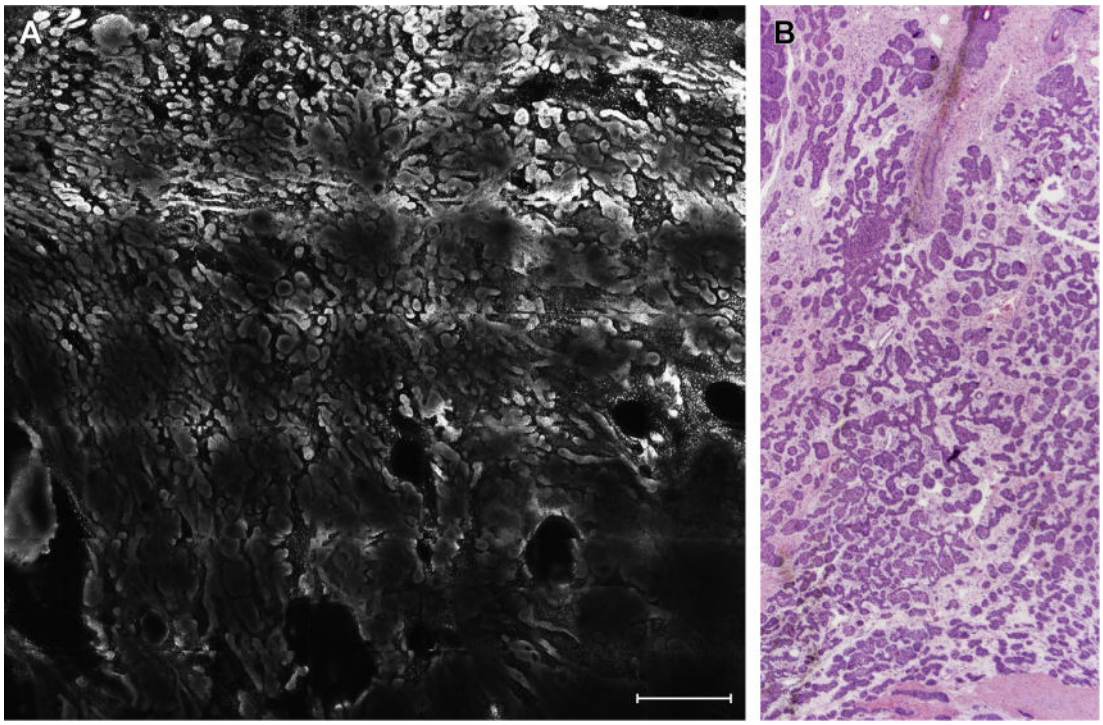

Fig. 3.

(*A*) Highly fluorescent basaloid tumor islands sharply demarcated compared with background dermis (scale bar, 750 μm) and (*B*) their histologic correlates (hematoxylin-eosin, original magnification 2×).

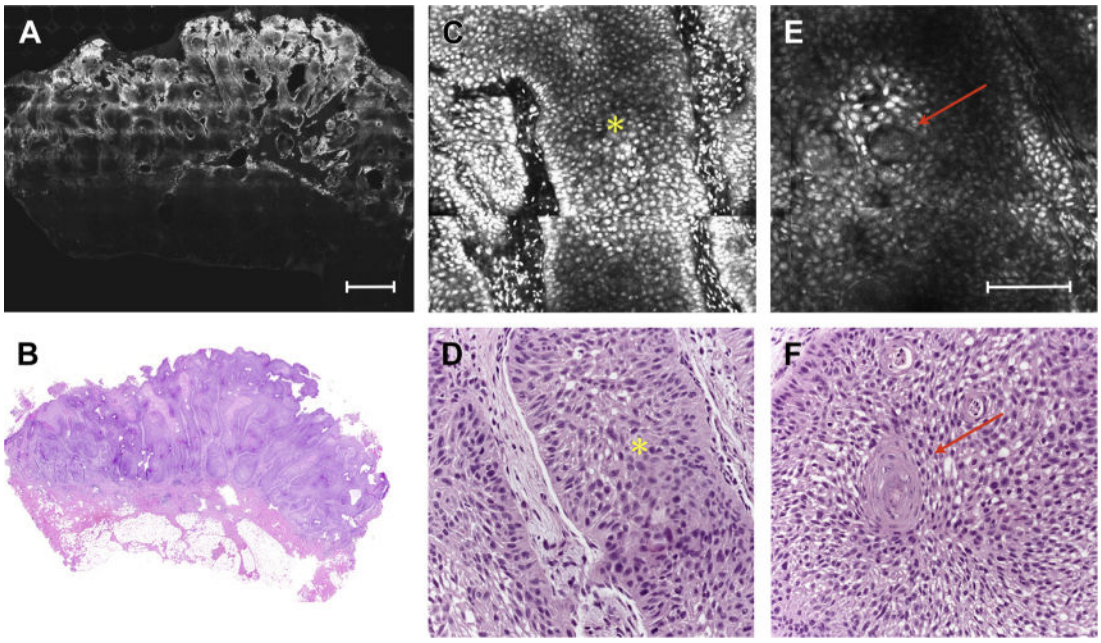

Fig. 4.

(*A*) FCM mosaic reveals a well-defined cutaneous squamous cell carcinoma silhouette with sharp demarcation and highly fluorescent areas (scale bar, 750 μm). (*B*) Corresponding histopathologic images showing a well-differentiated tumor (hematoxylin-eosin, original magnification 2×). (*C*) Detail of the tumor showing keratynocitic tongue (*asterisk*) and (*D*) its histologic correlates (*asterisk*) (hematoxylin-eosin, original magnification 10×). (*E*) Keratin pearls (*arrow*; scale bar, μm) and corresponding histologic image (*F*) (hematoxylin-eosin, original magnification 10×).

Table 1

Comparison of FCM studies

Study	Mosaics Evaluated, N	Confocal Technique	Se	Sp	PPV	NPV	Scanning Time (min) for 12 × 12 mm	Staining Time (min)	Staining Technique
Patel et al,[3] 2007	—	FCM	—	—	—	—	9	0.5–5	Acetic acid
Rajadhyaksha et al,[1] 2001	—	RCM	—	—	—	—	3.5	0.5	Acetic acid
Gareau et al,[11] 2009	30	RCM	—	—	—	—	9	0.5–5	Acetic acid
Schüle et al,[12] 2009	284	FCM	0–89	29–89	—	—	—	2	Citric acid
Ziefle et al,[13] 2010	312	FCM	82	61	66.7	78	3	3.5	Acetic acid + toluidine blue
Al-Arashi et al,[16] 2007	37	FCM, RCM	—	—	—	—	—	2	Toluidine blue, methylene blue
Gareau et al,[17] 2008	50	FCM	—	—	—	—	9	0.5	Acridine orange
Gareau et al,[18] 2009 Karen et al,[19] 2009	48	FCM	96.6	89.2	93	94.7	9	0.3	Acridine orange
Larson et al,[23] 2013	17	FCM strip	94	94	—	—	<2	0.3	Acricine orange
Bennàssar et al,[29] 2014	150	FCM	88	99	98	97	3	0.3	Acridine orange
Longo et al,[30] 2014	35	FCM	94.9	96.8	—	—	3	0.3	Acridine orange

Abbreviations: NPV, negative predictive value; PPV, positive predictive value; Se, sensitivity; Sp, specificity.